High-Resolution Mass Spectrometry Screening of Wastewater Effluent for Micropollutants and Their Transformation Products during Disinfection with Performic Acid

Maolida Nihemaiti, Nina Huynh, Romain Mailler, Perrine Mèche-Ananit, Vincent Rocher, Rachid Barhdadi, R. Moilleron, Julien Le Roux

ACS ES&T Water

pubs.acs.org/estwater

Article

High-Resolution Mass Spectrometry Screening of Wastewater Effluent for Micropollutants and Their Transformation Products during Disinfection with Performic Acid

Maolida Nihemaiti,[#] Nina Huynh,[#] Romain Mailler, Perrine Mèche-Ananit, Vincent Rocher, Rachid Barhdadi, Régis Moilleron, and Julien Le Roux*

Cite This: https://doi.org/10.1021/acsestwater.2c00075

Read Online

ACCESS | Metrics & More | Article Recommendations | Supporting Information

ABSTRACT: Performic acid (PFA) is an emerging disinfectant applied for full-scale disinfection of wastewater effluent. While many studies have focused on assessing the microbial water quality during PFA disinfection, studies on the ability of PFA to oxidize organic micropollutants are still scarce. In this study, nontarget screening of wastewater secondary effluent during PFA treatment was performed using liquid chromatography−high-resolution mass spectrometry. A low dose (2 mg/L) of PFA was able to affect the organic matter composition within a short exposure time (10 min). Multivariate analysis as well as suspect screening indicated that PFA oxidation largely reduced the intensities of micropollutants with a tertiary amine moiety and led to the formation of their mono-oxygenated derivatives, *N*-oxides, a class of transformation products that are known as biologically stable but whose impact on aquatic organisms still needs to be assessed. Mechanistic studies were conducted on selected micropollutants (i.e., lidocaine, amisulpride, tramadol, and clarithromycin). The minimum apparent second-order rate constant of PFA with lidocaine was determined as 7.54 M^{-1} s^{-1} at pH 8.0. Lidocaine was mainly converted (~95%) into its *N*-oxide via direct oxygen transfer from PFA. Overall results revealed a strong electrophilic reactivity of PFA toward electron-rich moieties (e.g., amines) of micropollutants.

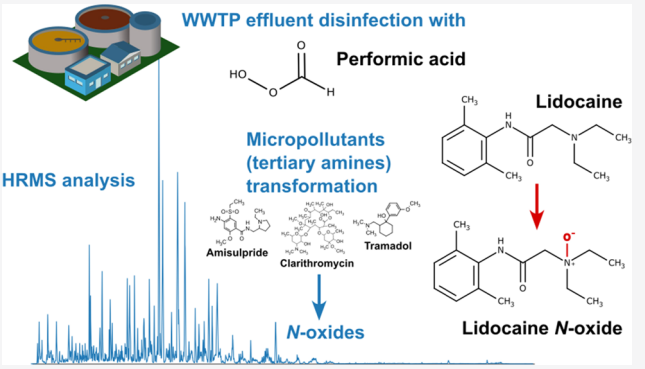

KEYWORDS: *peracids, trace organic chemicals, transformation products, wastewater disinfection, N-oxide, lidocaine*

1. INTRODUCTION

Organic aliphatic peracids such as peracetic acid (PAA, CH_3COOOH) and performic acid (PFA, HCOOOH) have been widely applied as oxidizing agents in chemical production, as disinfectants in food processing and medical field, and as biocides in the paper and pulp industry.[1−3] PAA has also been used in wastewater treatment since the late 1980s as an alternative to the conventional chlorine-based disinfectants.[3] More recently, PFA was tested for the disinfection of primary,[4] secondary,[5,6] and tertiary effluents of wastewater,[7] as well as the combined sewer overflows.[8] Several cities in Europe (e.g., Venice, Paris, and Berlin) are currently applying PFA at the full scale to disinfect wastewater effluents before discharge to surface water.[9,10] Some studies documented PFA to be more potent than PAA for the inactivation of *Escherichia coli* (*E. coli*) and enterococci.[7,8,11,12] The required dose of PFA varies depending on the site and the water matrix. A low dose of PFA (e.g., 0.8 mg/L for 18 min) was reported to enable 3-log reduction of *E. coli* in secondary wastewater effluent,[9] while another study reported 2-log reduction of *E. coli* in wastewater upon disinfection by 1 mg/L of PFA for 10−30 min.[13]

PFA is notably less stable than PAA and is thus produced on-site based on a reversible reaction between hydrogen peroxide (H_2O_2) and formic acid (eq 1), which can be catalyzed by mineral acids (e.g., sulfuric acid):[14]

$$HCOOH + H_2O_2 \leftrightarrow HCOOOH + H_2O \quad (1)$$

No genotoxic and mutagenic effects were observed in secondary effluent of municipal wastewater after PFA disinfection (0.6−1.5 mg/L).[15] The adsorbable organic halogens (AOX) formed during PFA disinfection were found to be substantially lower than PAA and chlorine under comparable disinfection levels (1 mg/L for 10 min), indicating that the formation of halogenated disinfection byproducts (e.g., through the reactions between oxidant species and

Received: February 11, 2022
Revised: June 13, 2022
Accepted: June 14, 2022

bromide or iodide ions) was limited.[5] PFA disinfections (1−3 mg/L, 10−30 min) of wastewater effluents were reported to have a negligible effect on the formation of trihalomethanes, haloacetonitriles, and *N*-nitrosamines.[9,10] However, detailed studies on the overall chemical characterization of wastewater, particularly the fate of organic micropollutants during PFA disinfection are still rare. The knowledge about PFA reactivity with organic micropollutants and organic matter in wastewater should be extended.

The treatments in conventional wastewater treatment plants (WWTPs) are generally not sufficient to completely remove micropollutants,[16] which can be further transformed during subsequent disinfection processes. Target and suspect screenings are the common approach to analyze micropollutants and their known transformation products.[17,18] However, the number of compounds investigated using these methods is often limited by the availability of reference standards or mass spectral database.[19] Nontarget screening combined with liquid chromatography−high resolution mass spectrometry (LC−HRMS) has emerged in recent years to comprehensively characterize organic substances in complex water matrices.[20,21] The high mass accuracy, isotope pattern, and MS/MS fragments obtained during nontarget screening stimulate the (tentative) identification of unknown compounds.[22] Furthermore, various statistical approaches that are used to interpret nontarget data allow the prioritization of the compounds of interest.[22] Such approaches (e.g., principal component analysis) were recently applied to investigate the effect of wastewater (e.g., biodegradation and ozonation)[23,24] and drinking water (e.g., advanced oxidation)[25] treatment processes on micropollutants and their transformation products.

The aim of this study was to investigate the impact of PFA oxidation on the chemical composition of wastewater. The WWTP effluent samples were treated with PFA at different doses and analyzed using LC−HRMS. Nontarget screening was first performed to generally characterize the samples. Multivariate statistics were then applied to prioritize the nontarget compounds that were most discriminating during treatment. Lidocaine *N*-oxide was found to be one of the transformation products that were increased significantly by PFA oxidation. Therefore, suspect screening of wastewater samples was performed for the selected tertiary amines and their *N*-oxides. Detailed experiments on the PFA oxidation of selected micropollutants were conducted in buffered pure water to confirm the formation of *N*-oxides and to understand the reaction mechanism of PFA oxidation.

2. MATERIALS AND METHODS

2.1. Chemical Reagents. All chemicals were of analytical grade and used as received without further purification. Amisulpride, clarithromycin, lidocaine, tramadol hydrochloride, clarithromycin *N*-oxide, sulfuric acid (98%), *tert*-butanol (>99.5%), and hydrogen peroxide (30%) were supplied from Sigma-Aldrich. Amisulpride *N*-oxide, lidocaine *N*-oxide, and tramadol *N*-oxide were obtained from Toronto Research Chemicals. Formic acid (99%) was purchased from Biosolve.

2.2. Preparation and Quantification of PFA. PFA was prepared based on the two-step Kemira (KemConnect DEX) preparation protocol as described previously.[10] Briefly, the acidified formic acid was first prepared by spiking 1 mL of sulfuric acid (98%) into 10 mL of formic acid (99%). Hydrogen peroxide (H_2O_2, 3.5 mL) was then slowly added into 1.5 mL of acidified formic acid. The mixture was allowed to react for 90 min in ice bath. The concentration of PFA in stock solution was quantified following a two-step titration. Residual H_2O_2 was first immediately titrated with $KMnO_4$ under acidic conditions, followed by the addition of KI. Iodide reacted with PFA to produce iodine, which formed an intense blue starch-iodine complex after the addition of the starch indicator. Sodium thiosulfate ($Na_2S_2O_3$) was then immediately applied to titrate the iodine until the disappearance of color. All solutions used for titration were ice cold to prevent the self-decomposition of PFA. Generally, the concentrations of PFA and H_2O_2 in equilibrium solution were about 10 and 17% by weight, respectively, comparable to previous studies.[4,5] The residual PFA during oxidation experiments was determined according to the ABTS (2,2′-azino-bis(3-ethylbenzothiazoline-6-sulfonic acid)) colorimetric method.[8,26,27] Briefly, 1 mL of aliquot of the diluted experimental solution (1:10 in ultrapure water) was mixed with 1 mL of acetic acid buffer (pH 3.5) and 1 mL of ABTS solution (0.1 g/L); it was allowed to react in the dark for 20 min and then analyzed using UV spectrometry at 415 nm.

2.3. PFA Treatment of Wastewater Effluent. Laboratory-scale and full-scale disinfections of wastewater effluent were conducted at the Seine Valenton wastewater treatment plant (SIAAP) located in Val-de-Marne, France, with a dry weather capacity of 600,000 m^3/day. The treatment trains include pretreatment steps (screening, sand trap), followed by primary settlement and two different low charge activated sludge treatment lines: first line performing nitrification and denitrification, completed by a tertiary physico-chemical removal of phosphorus, second line performing biological dephosphatation, nitrification, and denitrification. Grab samples of wastewater effluent (n = 3) were collected right before the discharge channel (mix of the two lines) from September to December 2018, and treated with PFA within 2 h of collection. PFA oxidation was carried out at the batch scale using 2 L aliquot of each wastewater sample under a constant stirring condition for 10 min. The initial dose of PFA was in the range of 1−100 mg/L. Wastewater effluent samples (n = 3) during full-scale disinfection by 0.8−2.5 mg/L PFA (C·t of 28.3−74.2 ppm·min) were also collected. The residual oxidant was immediately quenched with excess sodium thiosulfate. Samples were stored at 4 °C and extracted prior to LC−HRMS analysis within 24 h.

2.4. Sample Pretreatment. Wastewater samples treated using PFA were filtered through a 0.7 μm glass fiber filter (Whatman). A sample volume of 1 L was acidified to pH 6.5 with sulfuric acid and spiked with a mixed solution of isotope-labeled internal standards (i.e., bisphenol A-d6, 4-*n*-octylphenol-d17, 4-octylphenol-diethoxylate, and propylparaben-d4, 5 μg/L each). These internal standards were used to verify the intra-sequence variability and to correct the peak areas across samples accordingly. At least one blank sample with ultrapure water was prepared in the same way. Samples were enriched (concentration factor = 1000) with an automated solid-phase extraction (SPE) system (Dionex AutoTrace, Thermo Scientific) coupled with in-house filled multilayer SPE cartridges comprising Oasis HLB (Waters), isolute ENV+ (Biotage), Strata-X-AW (Phenomenex), and Strata-X-CW (Phenomenex).[28] The SPE cartridges were conditioned with 10 mL of methanol and 10 mL of ultrapure water. After the extraction, the cartridges were dried with nitrogen for 30 min, and the analytes were eluted with 6 mL of basic (1.4% of 35%

https://doi.org/10.1021/acsestwater.2c00075
ACS EST Water XXXX, XXX, XXX−XXX

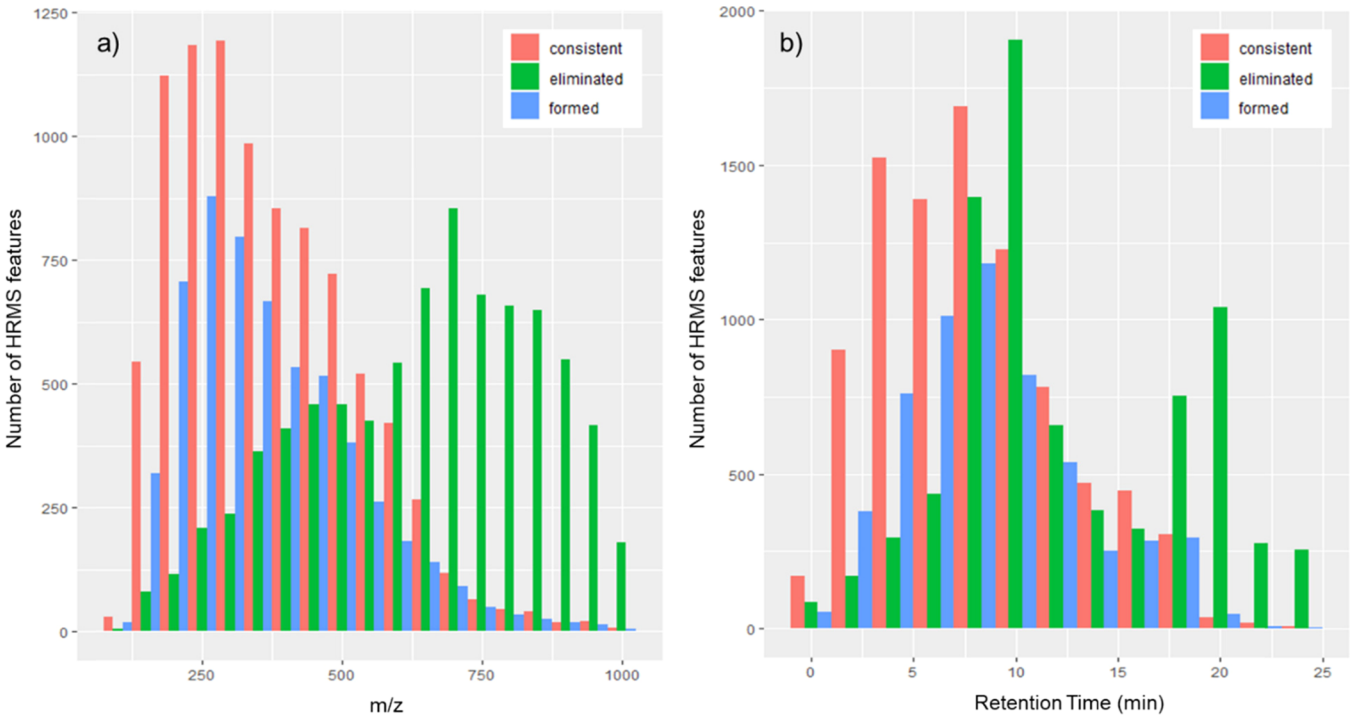

Figure 1. Distribution of the (a) m/z values and (b) retention times of HRMS features (ESI+ mode) from the average of three laboratory-scale experiments (initial [PFA] = 2 mg/L, contact time = 10 min). *Eliminated*, *formed*, and *consistent* categories were obtained by calculating the fold change value of each HRMS feature (the area after PFA oxidation divided by the area before oxidation).

ammonia) followed by 3 mL of acidic (1.7% of 98% formic acid) mixtures of methanol/ethyl acetate (50:50, v:v). The extract was then dried under a gentle nitrogen stream and reconstituted with 1 mL mixture of methanol and ultrapure water (20:80, v:v). All extracts were filtered through a 0.2 μm PTFE filter prior to LC−HRMS analysis. This extraction procedure showed good performances to recover a large range of micropollutants in target and nontarget screening compared to several other phases.[29,30]

2.5. PFA Oxidation of Selected Micropollutants. Experiments were conducted in amber glass bottles at room temperature (22 ± 2 °C). A 10 mL, 5 μM individual solution of each compound (i.e., lidocaine, amisulpride, tramadol, and clarithromycin) was prepared in 50 mM phosphate (pH = 6.2−8.0) or 10 mM borate buffer (pH = 9.0). Oxidation experiments were initiated by spiking the predetermined volume (26 μL−1.3 mL) of the diluted PFA stock (1:100 in ultrapure water) into this solution. The initial concentration of PFA was in the range of 2−100 mg/L. An experiment was performed with the addition of 100 mM *tert*-butanol to quench hydroxyl radicals potentially present in the solution and to study their possible contribution to the oxidation reaction. Samples (0.5 mL) were periodically withdrawn and quenched with excess sodium thiosulfate (10 μL of 0.1 M $Na_2S_2O_3$ in the case of 2−30 mg/L PFA and 10 μL of 1.0 M $Na_2S_2O_3$ in the case of 50−100 mg/L PFA). Samples were directly transferred to glass vials and injected to LC−HRMS and HPLC−UV within 24 h without further enrichment.

2.6. Instrumental Analysis. Samples were analyzed using an ultrahigh-performance liquid chromatography (UPLC) coupled with a high-resolution ion mobility time-of-flight mass spectrometry (Vion IMS-QTof, Waters) and equipped with an electrospray ionization (ESI) source. The chromatographic separation was achieved on an ACQUITY UPLC-BEH C18 column (1.7 μm, 2.1 × 100 mm, Waters) with gradient elution of ultrapure water (A) and acetonitrile (B) each containing 0.1% of formic acid as follows: 0−1 min: 2% B, 1−26 min: 2 to 98% B, 26−31 min: 98% B, 31−34 min: 98 to 2% B. The column temperature was set at 40 °C. Exactly 10 μL of the sample was injected at a flow rate of 450 μL/min. Separate runs were performed in positive and negative ionization modes with 0.8 kV and 2.5 kV capillary voltage, respectively. The source temperature was set at 120 °C (positive mode) and 100 °C (negative mode). The cone gas flow rate was 50 L/h. Desolvation gas flow rates were 1000 L/h (positive mode) and 600 L/h (negative mode). Data were collected in the m/z range of 100−1000 in sensitive mode (nominal resolution of 30,000 at m/z 556.2779). Two sets of data were recorded: low energy (6 V) and high collision ramp energy (20−56 V).

The quantification of lidocaine, amisulpride, tramadol, and their *N*-oxides during PFA oxidation in buffered pure water was performed using a HPLC instrument coupled with a diode array detector (DAD, SPD-M20A, Shimadzu) and an Ascentis Express C18 column (2.7 μm, 4.6 × 100 mm, Supelco). The mobile phase was composed of various isocratic mixtures of methanol and phosphate buffer (10 mM at pH 2.3). Compounds were analyzed at wavelengths with maximum UV absorbance. Details on HPLC-DAD analysis are provided in the Supporting Information (Table S1).

2.7. Data Processing. HRMS data were acquired and pretreated using UNIFI software (Waters). After peak detection, grouping of mass spectra and isotopes, and alignment, each detected feature was given a unique ID composed of its m/z, retention time, and drift time. The data were then exported as a csv table containing the ID of each feature and its respective peak area in each sample for further treatment with the R software.[31] The table was first filtered to only keep the features that were detected in all three injection

https://doi.org/10.1021/acsestwater.2c00075
ACS EST Water XXXX, XXX, XXX−XXX

replicates of a given sample. This filtered table was then employed for sample comparison and characterization. Suspect screening for parent compounds and their *N*-oxides was conducted using UNIFI with an in-house library. The compounds for which analytical standards were purchased were injected five times at three levels of concentration in order to gather data on their m/z, retention time, and drift time. Those properties were then used to compare acquired data on unknown samples, and suspect compounds were confirmed at level 1 when a match occurred within a tolerance of 5 ppm, retention time of 0.2 min, drift time 2%, and the presence of at least one fragment ion. For suspect screening without analytical standards, in silico fragmentation was carried out within UNIFI, and suspect compounds in unknown samples were confirmed at level 3 based on their m/z and the correspondence between the detected and in silico-generated fragments. The other compounds were searched based on their m/z and the correspondence between the detected and in silico-generated fragments.

3. RESULTS AND DISCUSSION

3.1. Nontarget Screening of Wastewater Effluent during PFA Oxidation. Nontarget screening was employed as a first approach to characterize the wastewater effluent samples treated by PFA. The overall impact of PFA was visualized through the classification of nontarget features into five categories determined by calculating the fold change in peak areas according to a previously published method.[32] Briefly, for each feature, the fold change (fc) was calculated by dividing the area in the sample after treatment by the area in the corresponding sample before PFA treatment. Depending on the result, the feature was assigned to the *eliminated* ($0.0 < fc < 0.2$), *partially removed* ($0.2 < fc < 0.5$), *consistent* ($0.5 < fc < 2.0$), *increased* ($2.0 < fc < 5.0$), or *formed* ($fc > 0.5$) category (Table S2).

About 50% of features that were initially present in wastewater effluent in positive and negative ionization modes were still detectable after 2 mg/L PFA oxidation for 10 min (Table S2). About 27 and 19% of features in positive and negative modes, respectively, were reduced by more than 80% or were not observed after PFA treatment, whereas 26 and 24% in positive and negative modes, respectively, were newly generated (i.e., oxidation byproducts). Furthermore, among the features that were present both before and after oxidation, 12 and 9% in positive and negative mode, respectively, had their peak areas reduced by 50 to 80%. Correspondingly, the overall signal intensities of all features were decreased by a factor of 2−4 after PFA oxidation (i.e., from 5.40×10^8 to 3.25×10^8 in positive mode and from 1.63×10^8 to 4.04×10^7 in negative mode), suggesting good ability of PFA to remove organic components, at least partially.

The average mass to charge values (m/z) and retention times of the eliminated features were higher than the formed features in both positive and negative ionization modes (Figures 1, S1, and Table S2), revealing the formation of smaller and more polar compounds from bigger and less polar ones. Features that were initially small and polar did not seem to be affected by PFA as they were mainly classified in the consistent category (Table S2). Overall results suggested that a low PFA exposure (2 mg/L for 10 min), as applied in tertiary disinfection, can alter the organic matter composition of the wastewater matrix.

Further classification of HRMS features found from nontarget screening of wastewater samples ($n = 12$) was carried out through Orthogonal Projections to Latent Structures Discriminant Analysis (OPLS-DA) and s-plot scores to select the most discriminant features during PFA treatment (0.8−2.5 mg/L, 10 min) at a laboratory and full scale. The OPLS-DA plot showed distinct clusters for samples before and after PFA oxidation, and the s-plot displayed the specific features of each group (Figure 2).

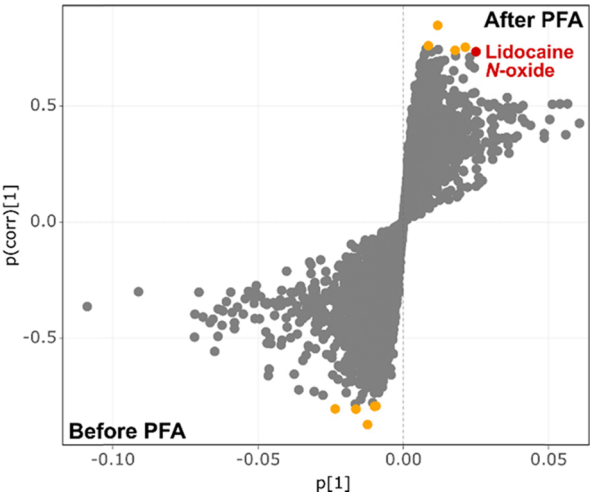

Figure 2. S-plot corresponding to the OPLS-DA model obtained during nontarget screening by comparing wastewater effluent before ($n = 6$, injected in triplicates) and after ($n = 6$, injected in triplicates) PFA treatment (initial [PFA] = 0.8−2.5 mg/L, contact time = 10 min). Features highlighted in yellow represent the most discriminant features (two features in "before PFA" are overlapped), including lidocaine *N*-oxide highlighted in red. Details on these features are given in Table S3.

Features with the highest couple of the p-corr value (correlation) and the loading value (covariance) were selected and tentatively identified using several online libraries (MassBank, Sigma-Aldrich, LGC Standard, NIST, and DrugBank as a part of the UNIFI system, as well as Chemspider and ForIdent). The five most discriminating nontarget features for each group (before and after PFA oxidation) are given in Table S3. Of these, a feature (m/z 251.1750, $[M + H] = C_{14}H_{23}N_2O_2$) was tentatively identified after PFA oxidation as lidocaine *N*-oxide based on the similarity of its exact mass, isotope pattern, and fragment ions to database. The presence of both lidocaine ($[M + H] = C_{14}H_{23}N_2O$, m/z 235.1804) and its *N*-oxide in wastewater samples was confirmed with corresponding analytical standards (Table S4). The peak area of lidocaine *N*-oxide gradually increased with the increasing PFA dose (except at 100 mg/L), while lidocaine tended to decrease, revealing the transformation of lidocaine to its *N*-oxide upon PFA oxidation (Figure 3).

3.2. Suspect Screening of Wastewater Effluent for *N*-Oxides and Their Precursors during PFA Oxidation. *N*-Oxides are the major products of deprotonated tertiary amines during biotransformation and ozonation[33,34] and known to be less biodegradable compared to their parent compounds.[18,35,36] To confirm the reactivity of PFA with tertiary amines to form *N*-oxides, suspect screening was performed to search for a total number of seven micropollutants comprising a tertiary amine

https://doi.org/10.1021/acsestwater.2c00075
ACS EST Water XXXX, XXX, XXX−XXX

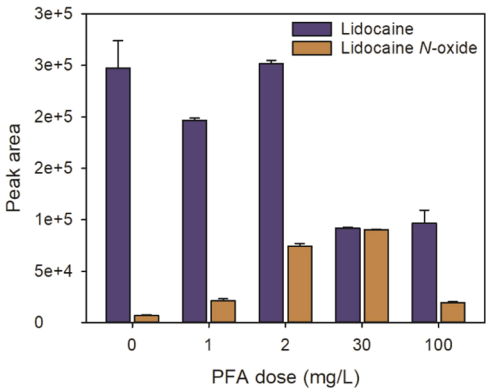

Figure 3. Peak area evolution of lidocaine and its *N*-oxide during PFA treatment (initial [PFA] = 0−100 mg/L, contact time = 10 min) of wastewater effluent. Error bars represent the standard deviations of triplicate analysis.

moiety and their corresponding *N*-oxides in wastewater (Table S4). Among those, amisulpride, clarithromycin, lidocaine, tramadol, and their corresponding *N*-oxides were confirmed at level 1 (from the injection of analytical standards) while other micropollutants were confirmed at level 3. The peak areas of all precursors were reduced during PFA treatment (2 mg/L, 10 min), whereas their corresponding *N*-oxides (except clarithromycin *N*-oxide and tramadol *N*-oxide) exhibited increasing formation, suggesting that PFA leads to the formation of *N*-oxides in wastewater.

3.3. Transformation Mechanisms of Selected Micropollutants by PFA. Detailed experiments on the oxidation of selected micropollutants were performed in buffered pure water to investigate the reaction mechanism of PFA.

3.3.1. Lidocaine. Control experiments were first conducted to study the effect of H_2O_2 on lidocaine. As an example, Figure S2 shows that 33 mg/L of H_2O_2, which was generally present in 10 mg/L PFA solution, had no impact on lidocaine in the pH range of 6.0−9.0. Furthermore, the presence of free radicals (including hydroxyl and peroxyl radicals) has been suggested during the decomposition of PFA and other peracids.[37,38] The addition of 0.1 M of *tert*-butanol had no impact on the degradation of lidocaine and formation of its *N*-oxide (Figure S3), indicating no involvement of hydroxyl radicals. Lidocaine was gradually degraded when applying various doses of PFA (Figure 4a). Approximately 20% of lidocaine was removed in 10 min by 5 mg/L of PFA at pH 8.0, whereas 80% of removal was achieved in 10 min when 30 mg/L of PFA was applied. Lidocaine was not degraded further when the reaction time was above 15 min (Figure 4a). This can be explained by the insufficient amount of residual PFA in the solution. Less than 5% of initial PFA (10 mg/L) was left within 20 min at pH 8.0. It was reported that PFA rapidly decomposes to CO_2 and H_2O in aqueous solution.[14,39,40] In this study, the first 6 min of reaction was considered when calculating the kinetic rate constants (Figure 4b), where the residual PFA was always in excess (>10 times) than lidocaine, and the degradation of lidocaine followed first-order kinetics. The observed-rate constant (min^{-1}), k_{obs}, which was derived from the slope of ln (C/C_0) versus time (Figure 4b), exhibited strong linearity with initial concentration of PFA (Figure 4b, inset), indicating that the overall reaction can be described by second-order reaction kinetics (eqs 2 and 3), yielding an apparent second-order rate constant, k_{app}, of 7.54 ± 0.90 M^{-1} s^{-1} at pH 8.0.

$$\frac{d[\text{lidocaine}]}{dt} = -k_{obs}[\text{lidocaine}] \quad (2)$$

$$\frac{d[\text{lidocaine}]}{dt} = -k_{app}[\text{lidocaine}][\text{PFA}] \quad (3)$$

Lidocaine was degraded faster at pH 8.0 than pH 7.0 (i.e., k_{app} of 2.76 ± 0.37 M^{-1} s^{-1}, Figure S4) likely due to the higher proportion (i.e., 0.65 vs 0.15, Figure S5) of the deprotonated lidocaine at pH 8.0 than pH 7.0 (pK_a = 7.75, www.chemaxon.com), where the deprotonated tertiary amine moiety can be easily attacked by PFA to produce the *N*-oxide. However, the k_{app} value might be slightly underestimated considering the self-decomposition of PFA within 6 min. Therefore, the k_{app} value here (i.e., 7.54 ± 0.90 M^{-1} s^{-1} at pH 8.0) can be considered as the minimum reaction rate constant of PFA with lidocaine. The ABTS method applied in this study requires a long measuring time (i.e., 20 min), and thus did not allow to accurately follow the kinetics of PFA decay during lidocaine degradation experiments. Even though performed at pH 3.5 to ensure PFA stability, this method could still slightly underestimate the PFA concentration because of some autodecomposition within 20 min of measuring time. Conversely, it has also been demonstrated that the ABTS method can overestimate the concentration of PAA because of the oxidation by

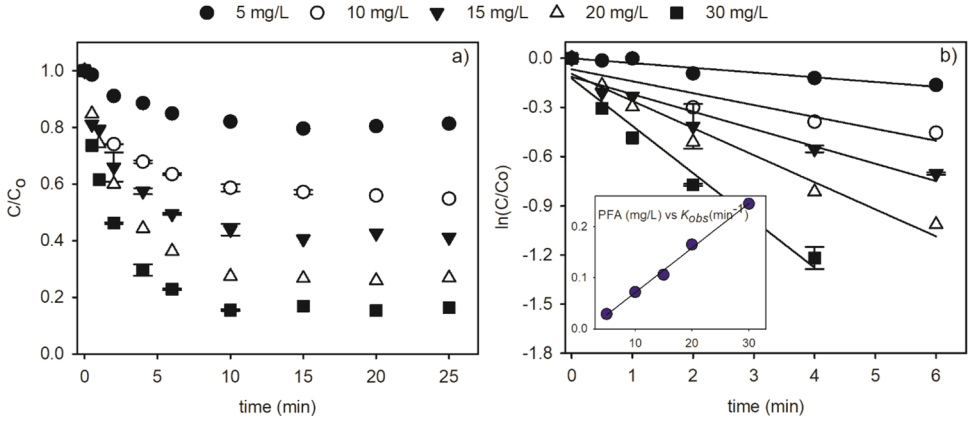

Figure 4. Degradation kinetics of lidocaine by PFA oxidation. Inset: k_{obs} versus initial concentration of PFA (initial [PFA] = 5−30 mg/L, initial [lidocaine] = 5 μM, 50 mM of phosphate buffer at pH 8.0). Error bars represent the standard deviations of duplicate experiments.

https://doi.org/10.1021/acsestwater.2c00075
ACS EST Water XXXX, XXX, XXX−XXX

H_2O_2.[41] For future kinetic studies on PFA treatments, careful estimation of PFA concentration at every sampling point must be undertaken to obtain the most accurate value of k_{app}, for example, using the DPD method.[42] Preliminary experiments on the self-decomposition of PFA in phosphate buffer were conducted in this study using the DPD method (Figure S6), which indicated that about 70% of PFA (initial dose of 2 mg/L) can self-decay within 20 min at pH 8.0.

Lidocaine *N*-oxide was gradually formed with the degradation of lidocaine (Figure S7). Figure 5 shows the concentrations of residual lidocaine and its *N*-oxide at 10 min reaction time. The sum of the molar concentrations of both compounds was almost stable despite different initial PFA doses, suggesting that lidocaine was mainly converted (~95%) to its *N*-oxide. Furthermore, PFA (0−100 mg/L) appeared to be unreactive with lidocaine *N*-oxide (Figure S8), revealing that *N*-oxide can pass through the PFA oxidation during wastewater disinfection as a persistent and final product. Two dealkylation products of lidocaine, that is, $C_{12}H_{18}N_2O$ (m/z 207.1487) and $C_{10}H_{13}NO$ (m/z 164.1068), were also observed during HRMS analysis, intensities of which increased with PFA exposure (Figure S9, mass spectra and intensity). As opposed to experiments in buffered pure water, complete conversion of lidocaine to its *N*-oxide was not observed at high PFA doses applied to real wastewater effluent. As shown in Figure 3, the formation of lidocaine *N*-oxide was reduced at 100 mg/L PFA compared to 30 mg/L PFA, even in the presence of residual lidocaine. This was possibly related to the involvement of other oxidation processes in the complex water matrix at a high PFA dose (e.g., Fenton reaction because of the addition of a high dose of H_2O_2 along with PFA), which would require further investigation.

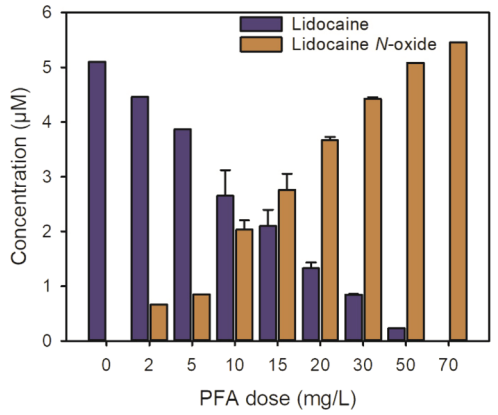

Figure 5. Concentrations of lidocaine *N*-oxide and residual lidocaine at 10 min reaction time (initial [PFA] = 0−70 mg/L, initial [lidocaine] = 5 μM, 50 mM of phosphate buffer at pH 8.0). Error bars represent the standard deviations of duplicate experiments.

The degradation pathways of lidocaine are proposed in Scheme 1. The overall reaction mechanism is similar to the oxidation of tertiary amines by ozone.[43,44] PFA attacks the lone pair electrons of nitrogen and forms *N*-oxide (P1, Scheme 1) as the major product by transferring its distal oxygen in the peroxide bond. The oxygen-transfer reactions were also observed from other oxidants incorporating peroxide bonds, such as PAA and peroxymonosulfate.[45−47] The direct electron transfer, as a minor transfer pathway, initiates the formation of amine radical cation and subsequent carbon-centered radical, which rapidly hydrolyzes into dealkylation products (P2 and P3, Scheme 1).

3.3.2. Amisulpride, Tramadol, and Clarithromycin. Amisulpride and tramadol were also mainly degraded to their *N*-oxides, but their degradation rates were much slower than lidocaine. Less than 0.1 μM of *N*-oxides were formed from amisulpride and tramadol (both 5 μM) at pH 8.0 by 10 mg/L of PFA oxidation for 10 min, whereas about 1.9 μM of lidocaine *N*-oxide can be formed at this PFA dose. This is likely related to the higher pK_a values of both compounds (pK_a = 8.28 for amisulpride and 9.23 for tramadol, www.chemaxon.com) than lidocaine. The deprotonated fractions of amisulpride (i.e., 0.35, Figure S5) and tramadol (i.e., 0.06, Figure S5) were much lower than that of lidocaine (i.e., 0.65) at pH 8.0 The pK_a of PFA (i.e., 7.1 at 19.5 °C)[48] could also play a role in those differences; however, data on the peracids reactivity at different pHs are still scarce. A few similar studies available for PAA did not clearly show a difference in reactivity depending on PAA species: it was more reactive under acidic conditions with β-lactamines[49] and amino acids[50] but more reactive under alkaline conditions with other organic

Scheme 1. Proposed Transformation Pathways of Lidocaine during PFA Oxidation

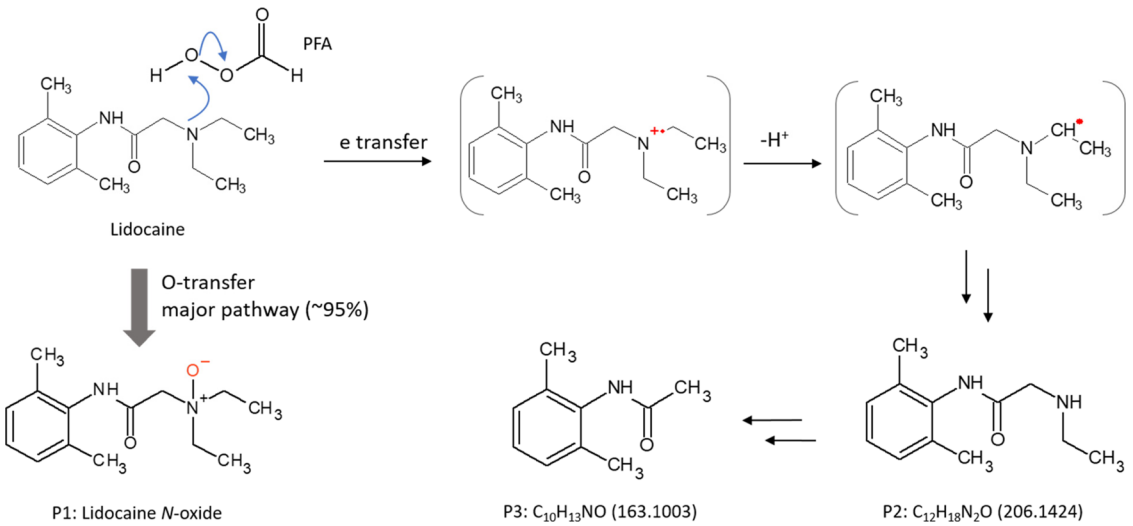

https://doi.org/10.1021/acsestwater.2c00075
ACS EST Water XXXX, XXX, XXX−XXX

compounds such as norfloxacine.[51] Analogous to lidocaine, PFA oxidation also resulted in the dealkylation of tertiary amines in amisulpride and tramadol, which was proved by the detection of dealkylation products during HRMS analysis, such as $C_{15}H_{23}N_3O_4S$ (m/z 342.1483, Figure S10a) from amisulpride and $C_{15}H_{23}NO_2$ (m/z 250.1804, Figure S10b) from tramadol (proposed formation pathways in Figure S11). Clarithromycin and its *N*-oxide were not quantified in this study. Nevertheless, the HRMS signal intensity of clarithromycin was gradually reduced with an elevated PFA dose at pH 8.0, leading to the formation of its *N*-oxide (Figure S12). Two additional transformation products (P1: m/z 588.3739, $C_{30}H_{53}NO_{10}$ and P2: m/z 606.3850, $C_{30}H_{53}NO_{11}$) were also found by HRMS analysis (Figure S13), which were proposed to be produced by the cleavage of the deoxysugar moiety in clarithromycin and its *N*-oxide (Figure S14). However, their HRMS signal intensities were 2 orders of magnitude lower than clarithromycin *N*-oxide (Figure S12).

4. CONCLUSIONS

PFA is increasingly applied for the disinfection of wastewater effluent because of its high efficacy to inactivate microorganisms and the low potential to produce regulated disinfection byproducts. However, there is still a large knowledge gap in terms of its reaction mechanism. Results from HRMS-based nontarget screening indicated that PFA disinfection at a short exposure time (e.g., 2 mg/L, 10 min) can reduce the total intensity of nontarget compounds in the secondary effluent of wastewater. The evolution of compounds after PFA oxidation, however, suggested that it can stimulate the generation of smaller and more polar oxidation byproducts from bigger and less polar molecules. The nontarget features were prioritized via OPLS-DA and s-plot, and lidocaine *N*-oxide was found as the compound of interest with significant intensity change upon PFA disinfection. Suspect screening for seven other *N*-oxides confirmed their formation in wastewater by PFA treatment, in line with the reduction of their parent compounds. Detailed experiments in buffered pure water suggested that lidocaine is mainly transformed to its *N*-oxide by oxygen-addition, with a minor formation of the dealkylation products and no contribution of both H_2O_2 and hydroxyl radicals. Comparable transformation mechanisms were also found from the PFA oxidation of amisulpride, tramadol, and clarithromycin. *N*-oxides are known to be less biodegradable than their parent compounds, raising the question of their persistence in the environment.[18,35,36] Their removal during ozonation requires higher doses, and partial reformation of the parent compound has been observed in biological post-treatment.[52] Little is known about their toxicity, and their potential impact on aquatic organisms relatively to their parent compound still needs to be assessed. While this family of molecules was significantly present in the oxidized samples, *N*-oxides do not follow the general trend observed during PFA oxidation (i.e., the generation of smaller and more polar compounds). Further efforts should be made to identify PFA-related polar oxidation byproducts. Results from this work, however, suggest the selective reactivity of PFA toward amine moieties. Similar mechanistic studies should be extended to other micropollutants incorporating electron-rich sites (e.g., unsaturated double bonds, reduced sulfur, and phenolic groups). Deriving kinetic rate constants for PFA reactivity with specific classes of organic compounds will enable their quantitative comparison with other oxidants such as PAA (as recently reviewed by Kim and Huang[45]) or ozone.[53] Results from this study also reveal that PFA might be highly reactive with the nitrogen-containing biomolecules in cells (e.g., peptides, proteins in membrane), which could help understand the inactivation mechanism of microorganisms by PFA at the molecular level.

■ ASSOCIATED CONTENT

Supporting Information

The Supporting Information is available free of charge at https://pubs.acs.org/doi/10.1021/acsestwater.2c00075.

Additional analytical details, self-decomposition kinetics of PFA and additional kinetics results, species distribution diagrams of selected micropollutants, HRMS global characterization, HRMS identification and detection results, HRMS spectra of micropollutants and their transformation products (from analytical standards and wastewater samples), and additional transformation pathways (PDF)

■ AUTHOR INFORMATION

Corresponding Author

Julien Le Roux − *Univ Paris-Est Creteil, LEESU, F-94010 Creteil, France; Ecole des Ponts, LEESU, F-77455 Champs-sur-Marne, France;* orcid.org/0000-0003-0245-8536; Phone: +33(0)182392080; Email: julien.le-roux@u-pec.fr

Authors

Maolida Nihemaiti − *Univ Paris-Est Creteil, LEESU, F-94010 Creteil, France; Ecole des Ponts, LEESU, F-77455 Champs-sur-Marne, France*

Nina Huynh − *Univ Paris-Est Creteil, LEESU, F-94010 Creteil, France; Ecole des Ponts, LEESU, F-77455 Champs-sur-Marne, France*

Romain Mailler − *Service Public de l'assainissement Francilien (SIAAP), Direction Innovation Environnement, F-92700 Colombes, France;* Present Address: Suez TI, Innovation and Technical Direction, 16 place de l'Iris, 92040 Courbevoie, France

Perrine Mèche-Ananit − *Service Public de l'assainissement Francilien (SIAAP), Direction Innovation Environnement, F-92700 Colombes, France;* Present Address: Direction de l'eau, centre assainissement, Bordeaux Métropole, Esplanade Charles-de-Gaulle, 33045 Bordeaux Cedex, France

Vincent Rocher − *Service Public de l'assainissement Francilien (SIAAP), Direction Innovation Environnement, F-92700 Colombes, France*

Rachid Barhdadi − *Univ Paris-Est Creteil, LEESU, F-94010 Creteil, France; Ecole des Ponts, LEESU, F-77455 Champs-sur-Marne, France*

Régis Moilleron − *Univ Paris-Est Creteil, LEESU, F-94010 Creteil, France; Ecole des Ponts, LEESU, F-77455 Champs-sur-Marne, France*

Complete contact information is available at: https://pubs.acs.org/10.1021/acsestwater.2c00075

Author Contributions

#M.N. and N.H. contributed equally to this work.

Notes

The authors declare no competing financial interest.

https://doi.org/10.1021/acsestwater.2c00075
ACS EST Water XXXX, XXX, XXX−XXX

■ ACKNOWLEDGMENTS

The research leading to these results has received funding from the "People" Programme (Marie Curie Actions) of the European Union's Seventh Framework Programme (FP7/2007-2013) under REA grant agreement no. PCOFUND-GA-2013-609102, through the PRESTIGE programme coordinated by Campus France. This work also received funding from the WaterOmics project (ANR-17-CE34-0009-01) and postdoctoral fellowship from Univ Paris-Est Creteil. The authors would like to thank Emmanuel Mebold and Emilie Caupos for their assistance with LC−MS analysis. The authors truly appreciate the valuable revision suggestions of anonymous reviewers.

■ REFERENCES

(1) Heinonen-Tanski, H.; Miettinen, H. Performic acid as a potential disinfectant at low temperature. *J. Food Process Eng.* **2010**, *33*, 1159−1172.
(2) Luukkonen, T.; Pehkonen, S. O. Peracids in water treatment: A critical review. *Crit. Rev. Environ. Sci. Technol.* **2017**, *47*, 1−39.
(3) Kitis, M. Disinfection of wastewater with peracetic acid: a review. *Environ. Int.* **2004**, *30*, 47−55.
(4) Gehr, R.; Chen, D.; Moreau, M. Performic acid (PFA): tests on an advanced primary effluent show promising disinfection performance. *Water Sci. Technol.* **2009**, *59*, 89−96.
(5) Karpova, T.; Pekonen, P.; Gramstad, R.; Öjstedt, U.; Laborda, S.; Heinonen-Tanski, H.; Chávez, A.; Jiménez, B. Performic acid for advanced wastewater disinfection. *Water Sci. Technol.* **2013**, *68*, 2090−2096.
(6) Ragazzo, P.; Chiucchini, N.; Piccolo, V.; Ostoich, M. A new disinfection system for wastewater treatment: performic acid full-scale trial evaluations. *Water Sci. Technol.* **2013**, *67*, 2476−2487.
(7) Luukkonen, T.; Heyninck, T.; Rämö, J.; Lassi, U. Comparison of organic peracids in wastewater treatment: Disinfection, oxidation and corrosion. *Water Res.* **2015**, *85*, 275−285.
(8) Chhetri, R. K.; Thornberg, D.; Berner, J.; Gramstad, R.; Öjstedt, U.; Sharma, A. K.; Andersen, H. R. Chemical disinfection of combined sewer overflow waters using performic acid or peracetic acids. *Sci. Total Environ.* **2014**, *490*, 1065−1072.
(9) Ragazzo, P.; Chiucchini, N.; Piccolo, V.; Spadolini, M.; Carrer, S.; Zanon, F.; Gehr, R. Wastewater disinfection: long-term laboratory and full-scale studies on performic acid in comparison with peracetic acid and chlorine. *Water Res.* **2020**, *184*, No. 116169.
(10) Rocher, V.; Azimi, S.; Mailler, R.; Rechdaoui-Guérin, S.; Mèche, P.; Pichon, S.; Goffin, A.; Bernier, J.; Roy, J.; Varrault, G.; Le Roux, J.; Huynh, N.; Nihemaiti, M.; Pigot, T.; Paulin, T.; Mouchel, J.-M.; Du Pasquier, D.; Paulic, L.; Angelescu, D. E.; Huynh, V.; Hausot, A.; Ragazzo, P.; Chiucchini, N. *Effectiveness of Disinfecting Wastewater Treatment Plant Discharges: Case of chemical disinfection using performic acid*. IWA Publishing, 2021.
(11) Maffettone, R.; Manoli, K.; Santoro, D.; Passalacqua, K. D.; Wobus, C. E.; Sarathy, S. Performic Acid Disinfection of Municipal Secondary Effluent Wastewater: Inactivation of Murine Norovirus, Fecal Coliforms, and Enterococci. *Environ. Sci. Technol.* **2020**, *54*, 12761−12770.
(12) Campo, N.; De Flora, C.; Maffettone, R.; Manoli, K.; Sarathy, S.; Santoro, D.; Gonzalez-Olmos, R.; Auset, M. Inactivation kinetics of antibiotic resistant Escherichia coli in secondary wastewater effluents by peracetic and performic acids. *Water Res.* **2020**, *169*, No. 115227.
(13) Mailler, R.; Mèche, P.; Rocher, V. What removals of pathogen indicators can be expected within large-scale wastewater treatment facilities in the context of wastewater reuse in Paris conurbation? *Water Sci. Technol.* **2021**, *83*, 781−791.
(14) Filippis, P. D.; Scarsella, M.; Verdone, N. Peroxyformic Acid Formation: A Kinetic Study. *Ind. Eng. Chem. Res.* **2009**, *48*, 1372−1375.
(15) Ragazzo, P.; Feretti, D.; Monarca, S.; Dominici, L.; Ceretti, E.; Viola, G.; Piccolo, V.; Chiucchini, N.; Villarini, M. Evaluation of cytotoxicity, genotoxicity, and apoptosis of wastewater before and after disinfection with performic acid. *Water Res.* **2017**, *116*, 44−52.
(16) Eggen, R. I. L.; Hollender, J.; Joss, A.; Schärer, M.; Stamm, C. Reducing the Discharge of Micropollutants in the Aquatic Environment: The Benefits of Upgrading Wastewater Treatment Plants. *Environ. Sci. Technol.* **2014**, *48*, 7683−7689.
(17) Deeb, A. A.; Stephan, S.; Schmitz, O. J.; Schmidt, T. C. Suspect screening of micropollutants and their transformation products in advanced wastewater treatment. *Sci. Total Environ.* **2017**, *601*−*602*, 1247−1253.
(18) Bourgin, M.; Beck, B.; Boehler, M.; Borowska, E.; Fleiner, J.; Salhi, E.; Teichler, R.; von Gunten, U.; Siegrist, H.; McArdell, C. S. Evaluation of a full-scale wastewater treatment plant upgraded with ozonation and biological post-treatments: Abatement of micro-pollutants, formation of transformation products and oxidation by-products. *Water Res.* **2018**, *129*, 486−498.
(19) Schymanski, E. L.; Singer, H. P.; Longrée, P.; Loos, M.; Ruff, M.; Stravs, M. A.; Ripollés Vidal, C.; Hollender, J. Strategies to Characterize Polar Organic Contamination in Wastewater: Exploring the Capability of High Resolution Mass Spectrometry. *Environ. Sci. Technol.* **2014**, *48*, 1811−1818.
(20) Schymanski, E. L.; Singer, H. P.; Slobodnik, J.; Ipolyi, I. M.; Oswald, P.; Krauss, M.; Schulze, T.; Haglund, P.; Letzel, T.; Grosse, S.; Thomaidis, N. S.; Bletsou, A.; Zwiener, C.; Ibáñez, M.; Portolés, T.; de Boer, R.; Reid, M. J.; Onghena, M.; Kunkel, U.; Schulz, W.; Guillon, A.; Noyon, N.; Leroy, G.; Bados, P.; Bogialli, S.; Stipaničev, D.; Rostkowski, P.; Hollender, J. Non-target screening with high-resolution mass spectrometry: critical review using a collaborative trial on water analysis. *Anal. Bioanal. Chem.* **2015**, *407*, 6237−6255.
(21) Gago-Ferrero, P.; Schymanski, E. L.; Bletsou, A. A.; Aalizadeh, R.; Hollender, J.; Thomaidis, N. S. Extended Suspect and Non-Target Strategies to Characterize Emerging Polar Organic Contaminants in Raw Wastewater with LC-HRMS/MS. *Environ. Sci. Technol.* **2015**, *49*, 12333−12341.
(22) Hollender, J.; Schymanski, E. L.; Singer, H. P.; Ferguson, P. L. Nontarget Screening with High Resolution Mass Spectrometry in the Environment: Ready to Go? *Environ. Sci. Technol.* **2017**, *51*, 11505−11512.
(23) Schollée, J. E.; Schymanski, E. L.; Avak, S. E.; Loos, M.; Hollender, J. Prioritizing Unknown Transformation Products from Biologically-Treated Wastewater Using High-Resolution Mass Spectrometry, Multivariate Statistics, and Metabolic Logic. *Anal. Chem.* **2015**, *87*, 12121−12129.
(24) Schollée, J. E.; Bourgin, M.; von Gunten, U.; McArdell, C. S.; Hollender, J. Non-target screening to trace ozonation transformation products in a wastewater treatment train including different post-treatments. *Water Res.* **2018**, *142*, 267−278.
(25) Brunner, A. M.; Bertelkamp, C.; Dingemans, M. M. L.; Kolkman, A.; Wols, B.; Harmsen, D.; Siegers, W.; Martijn, B. J.; Oorthuizen, W. A.; ter Laak, T. L. Integration of target analyses, non-target screening and effect-based monitoring to assess OMP related water quality changes in drinking water treatment. *Sci. Total Environ.* **2020**, *705*, No. 135779.
(26) Sode, F. Analytical methods for peroxo acids − a review. *Anal. Methods* **2019**, *11*, 3372−3380.
(27) Pinkernell, U.; Lüke, H.-J.; Karst, U. Selective Photometric Determination of Peroxycarboxylic Acids in the Presence of Hydrogen Peroxide. *Analyst* **1997**, *122*, 567−571.
(28) Kern, S.; Fenner, K.; Singer, H. P.; Schwarzenbach, R. P.; Hollender, J. Identification of Transformation Products of Organic Contaminants in Natural Waters by Computer-Aided Prediction and High-Resolution Mass Spectrometry. *Environ. Sci. Technol.* **2009**, *43*, 7039−7046.
(29) Huntscha, S.; Singer, H. P.; McArdell, C. S.; Frank, C. E.; Hollender, J. Multiresidue analysis of 88 polar organic micropollutants in ground, surface and wastewater using online mixed-bed multilayer solid-phase extraction coupled to high performance liquid chromatog-

https://doi.org/10.1021/acsestwater.2c00075
ACS EST Water XXXX, XXX, XXX−XXX

raphy−tandem mass spectrometry. *J. Chromatogr. A* **2012**, *1268*, 74−83.
(30) Huynh, N.; Caupos, E.; Soares Peirera, C.; Le Roux, J.; Bressy, A.; Moilleron, R. Evaluation of Sample Preparation Methods for Non-Target Screening of Organic Micropollutants in Urban Waters Using High-Resolution Mass Spectrometry. *Molecules* **2021**, *26*, 7064.
(31) R Core Team; *R: a language and environment for statistical computing*; R Foundation for Statistical Computing: Vienna, Austria, 2009.
(32) Bader, T.; Schulz, W.; Kümmerer, K.; Winzenbacher, R. LC-HRMS Data Processing Strategy for Reliable Sample Comparison Exemplified by the Assessment of Water Treatment Processes. *Anal. Chem.* **2017**, *89*, 13219−13226.
(33) Merel, S.; Lege, S.; Yanez Heras, J. E.; Zwiener, C. Assessment of N-Oxide Formation during Wastewater Ozonation. *Environ. Sci. Technol.* **2017**, *51*, 410−417.
(34) Gulde, R.; Meier, U.; Schymanski, E. L.; Kohler, H.-P. E.; Helbling, D. E.; Derrer, S.; Rentsch, D.; Fenner, K. Systematic Exploration of Biotransformation Reactions of Amine-Containing Micropollutants in Activated Sludge. *Environ. Sci. Technol.* **2016**, *50*, 2908−2920.
(35) Hubner, U.; von Gunten, U.; Jekel, M. Evaluation of the persistence of transformation products from ozonation of trace organic compounds - a critical review. *Water Res.* **2015**, *68*, 150−170.
(36) Seiwert, B.; Nihemaiti, M.; Bauer, C.; Muschket, M.; Sauter, D.; Gnirss, R.; Reemtsma, T. Ozonation products from trace organic chemicals in municipal wastewater and from metformin: peering through the keyhole with supercritical fluid chromatography-mass spectrometry. *Water Res.* **2021**, *196*, No. 117024.
(37) Rokhina, E. V.; Makarova, K.; Golovina, E. A.; Van As, H.; Virkutyte, J. Free Radical Reaction Pathway, Thermochemistry of Peracetic Acid Homolysis, and Its Application for Phenol Degradation: Spectroscopic Study and Quantum Chemistry Calculations. *Environ. Sci. Technol.* **2010**, *44*, 6815−6821.
(38) Shi, H.-C.; Li, Y. Formation of nitroxide radicals from secondary amines and peracids: A peroxyl radical oxidation pathway derived from electron spin resonance detection and density functional theory calculation. *J. Mol. Catal. A: Chem.* **2007**, *271*, 32−41.
(39) Santacesaria, E.; Russo, V.; Tesser, R.; Turco, R.; Di Serio, M. Kinetics of Performic Acid Synthesis and Decomposition. *Ind. Eng. Chem. Res.* **2017**, *56*, 12940−12952.
(40) Sun, X.; Zhao, X.; Du, W.; Liu, D. Kinetics of Formic Acid-autocatalyzed Preparation of Performic Acid in Aqueous Phase. *Chin. J. Chem. Eng.* **2011**, *19*, 964−971.
(41) Domínguez-Henao, L.; Turolla, A.; Monticelli, D.; Antonelli, M. Assessment of a colorimetric method for the measurement of low concentrations of peracetic acid and hydrogen peroxide in water. *Talanta* **2018**, *183*, 209−215.
(42) Cavallini, G. S.; de Campos, S. X.; de Souza, J. B.; Vidal, C. M. D. S. Comparison of methodologies for determination of residual peracetic acid in wastewater disinfection. *Int. J. Environ. Anal. Chem.* **2013**, *93*, 906−918.
(43) Lange, F.; Cornelissen, S.; Kubac, D.; Sein, M. M.; von Sonntag, J.; Hannich, C. B.; Golloch, A.; Heipieper, H. J.; Möder, M.; von Sonntag, C. Degradation of macrolide antibiotics by ozone: A mechanistic case study with clarithromycin. *Chemosphere* **2006**, *65*, 17−23.
(44) von Sonntag, C.; von Gunten, U. *Chemistry of Ozone in Water and Wastewater Treatment: From Basic Principles to Applications*; IWA Publishing, 2012.
(45) Kim, J.; Huang, C.-H. Reactivity of Peracetic Acid with Organic Compounds: A Critical Review. *ACS EST Water* **2021**, *1*, 15−33.
(46) Wang, Z.; Bush, R. T.; Sullivan, L. A.; Chen, C.; Liu, J. Selective Oxidation of Arsenite by Peroxymonosulfate with High Utilization Efficiency of Oxidant. *Environ. Sci. Technol.* **2014**, *48*, 3978−3985.
(47) Nihemaiti, M.; Permala, R. R.; Croué, J.-P. Reactivity of unactivated peroxymonosulfate with nitrogenous compounds. *Water Res.* **2020**, *169*, No. 115221.
(48) Everett, A. J.; Minkoff, G. J. The dissociation constants of some alkyl and acyl hydroperoxides. *Trans. Faraday Soc.* **1953**, *49*, 410−414.
(49) Zhang, K.; Zhou, X.; Du, P.; Zhang, T.; Cai, M.; Sun, P.; Huang, C.-H. Oxidation of β-lactam antibiotics by peracetic acid: Reaction kinetics, product and pathway evaluation. *Water Res.* **2017**, *123*, 153−161.
(50) Du, P.; Liu, W.; Cao, H.; Zhao, H.; Huang, C.-H. Oxidation of amino acids by peracetic acid: Reaction kinetics, pathways and theoretical calculations. *Water Res.: X* **2018**, *1*, 100002.
(51) Ao, X.-W.; Eloranta, J.; Huang, C.-H.; Santoro, D.; Sun, W.-J.; Lu, Z.-D.; Li, C. Peracetic acid-based advanced oxidation processes for decontamination and disinfection of water: A review. *Water Res.* **2021**, *188*, No. 116479.
(52) Zucker, I.; Mamane, H.; Riani, A.; Gozlan, I.; Avisar, D. Formation and degradation of N-oxide venlafaxine during ozonation and biological post-treatment. *Sci. Total Environ.* **2018**, *619−620*, 578−586.
(53) Lee, Y.; von Gunten, U. Quantitative structure−activity relationships (QSARs) for the transformation of organic micropollutants during oxidative water treatment. *Water Res.* **2012**, *46*, 6177−6195.

https://doi.org/10.1021/acsestwater.2c00075
ACS EST Water XXXX, XXX, XXX−XXX